

## Synthesis and Electrochemical Properties of Rhombohedral LiFePO<sub>4</sub>/C Microcrystals Via a Hydrothermal Route for Lithium Ion Batteries

Mohadese Rastgoo-Deylami<sup>1</sup>, Mehran Javanbakht<sup>1,2,\*</sup>, Mehdi Ghaemi<sup>2,3</sup>, Leila Naji<sup>1</sup>,  
Hamid Omidvar<sup>2,4</sup>, Mohammad Reza Ganjali<sup>5\*</sup>

<sup>1</sup>Department of Chemistry, Amirkabir University of Technology, Tehran, Iran

<sup>2</sup>Renewable Energy Research Center, Amirkabir University of Technology, Tehran, Iran

<sup>3</sup>Department of Chemistry, Science faculty, Golestan University, Gorgan, Iran

<sup>4</sup>Department of Mining and Metallurgical Engineering, Amirkabir University of Technology, Tehran, Iran

<sup>5</sup>Center of Excellence in Electrochemistry, University of Tehran, Tehran, Iran

\*E-mail: [mehranjavanbakht@gmail.com](mailto:mehranjavanbakht@gmail.com); [Ganjali@khayam.ut.ac.ir](mailto:Ganjali@khayam.ut.ac.ir)

Received: 25 July 2013 / Accepted: 12 December 2013 / Published: 23 March 2014

---

Lithium iron phosphate platelets are synthesized by a facile hydrothermal method at 160 °C using polyethylene glycol (PEG) as structure oriented agent and surface-modified reagent. Different samples were prepared by adding 2-32 vol. % polyethylene glycol (PEG) to the precursor solutions before heating. The structural and morphological properties of the resulting samples were investigated by means of X-ray diffraction (XRD) and scanning electron microscopy (SEM). The amounts of Fe<sup>3+</sup> and Li<sup>+</sup> were determined by spectrophotometric method and flame AAS, respectively. Results show that by increasing the PEG content from 2 to 8 vol. %, the morphology turned from rectangular platelets to single crystals with well-developed rhombohedral morphology. The electrochemical properties of samples were measured by the cyclic voltammetry (CV), electrochemical impedance spectroscopy (EIS) and galvanostatic charge-discharge cycling. According to the data obtained in this study, increasing PEG content, increase the Li/Fe ratio and enhance the electrochemical performance of LiFePO<sub>4</sub>/C samples. LiFePO<sub>4</sub>/C samples, prepared from the precursor solution having 32 vol. % PEG, shows much higher initial discharge capacity in the order of 143 mAh g<sup>-1</sup> at 0.1 C discharge rates. The latter represents phase of the ordered olivine structure with a thickness ranging from 550 nm to 2.5 μm. EIS revealed a smaller charge-transfer resistance and higher Li ion diffusivity. The increase in the initial discharge capacity should be correlated with decrease in particle size and increase in the degree of crystallization. Results of this work show that the morphologies of the lithium iron phosphate can be readily controlled by adding various amounts of PEG in the precursor solution. The approach, described in this work, may be used for further optimizing the preparation techniques and microstructures of rhombohedral LiFePO<sub>4</sub>/C composites.

---

**Keywords:** LiFePO<sub>4</sub>; Olivine; Li-ion battery; Hydrothermal; Platelets; Rhombohedral

## 1. INTRODUCTION

Progress in energy storage materials are special branch of chemist's capabilities to design new and better electrode materials for use in energy storage devices. In addition to high energy notions of sustainability, renewability and green chemistry must be taken in to consideration when selecting cathode materials for the advanced rechargeable batteries. Lithium-ion batteries are one of the great successes of modern materials electrochemistry due to their high energy density and good performance. In this regard, lithium iron phosphate ( $\text{LiFePO}_4$ ) has been recognized as a promising cathode material for Li batteries. Olivine type  $\text{LiMPO}_4$  (M=transition metal) is one of polyanionic compounds, such as NASICON  $\text{Li}_3\text{Fe}_2(\text{PO}_4)_3$  and monoclinic (or rhombohedral)  $\text{Fe}_2(\text{SO}_4)_3$ . The polyanionic compounds can be viewed as replacement of  $\text{O}^{2-}$  anions by larger size  $(\text{XO}_4)^{m-}$  polyanions such as  $\text{PO}_4^{3-}$ ,  $\text{SO}_4^{2-}$ ,  $\text{MoO}_4^{2-}$ , - and so forth.

$\text{LiFePO}_4$ , with a phospho-olivine structure (orthorhombic structure, *Pnma*), has been regarded as one of the most promising cathode materials. This material is environmentally benign and inexpensive with a theoretical capacity of  $170 \text{ mAh.g}^{-1}$ . Furthermore, it shows excellent thermal- and cycle stability due to structural similarity between charged/discharged states. These properties make it an attractive candidate for large scale batteries such as power source for plug-in hybrid electric vehicle (PHEV) [1-5]. Initially  $\text{LiFePO}_4$  was not a favorite as potential material for use as electrodes because of both poor electronic and ionic conductivity. The rate-determining step in the cycling process seems to be lithium diffusion through a diminishing  $\text{LiFePO}_4/\text{FePO}_4$  interface as lithium is reinserted into the  $\text{FePO}_4$  structure.

To obtain  $\text{LiFePO}_4$  with fine particles for high power purpose, it is essential to take advantages of solution synthetic route such as precipitation [6] sol-gel and hydrothermal methods [7-13]. In pioneering attempt, Whittingham and co-workers displayed the synthesis of  $\text{LiFePO}_4$  via hydrothermal reaction at  $120 \text{ }^\circ\text{C}$ , but the product showed a low electrochemical activity due to a severe displacement of Fe in Li site [9]. A following report by them demonstrated that the displacement of Fe and Li could be remarkably suppressed when arising temperature above  $180 \text{ }^\circ\text{C}$  [10]. However, the materials obtained do not show satisfactory electrochemical behavior, probably due to high particle growth rate [10,11] or the presence of impurities [12,13].

The properties of product could be tuned via optimization of experimental parameters such as temperature, pressure, concentration and additives. Additive are in general organic modifying surfactants or polymers, which can be either synthetic macromolecules with well-controlled architecture or natural polymers. Hydrophilic molecules, such as polyethylene glycol (PEG), have also been extensively used to control the growth and stability of mineral phases. PEG, due to its template assembly, is suggested to take part in the texture formation on seed surfaces and so modify the morphology of crystalline films.

The problem of olivine type  $\text{LiFePO}_4$  is its low electrical (electronic and ionic) conductivity, so electrochemical properties depend on charge/discharge rate and operating temperatures. These drawbacks, including lower operating voltage and poor rate capability, prevent the cathode material from commercial application. In order to overcome this drawback, many works have been done and it is found that reduction of particle size and increase in electronic conductivity by coating of conducting

agent are quite effective. Here, we report on the use of polyethylene glycol as both carbon source and as a structural directing agent to orient crystal growth template and to control the growth kinetics of  $\text{LiFePO}_4$ .

## 2. EXPERIMENTAL PART

### 2.1. Synthesis of plate-like $\text{LiFePO}_4$ samples

$\text{LiFePO}_4$  was prepared *via* the hydrothermal route using starting materials:  $\text{FeSO}_4 \cdot 7\text{H}_2\text{O}$ ,  $\text{H}_3\text{PO}_4$  and  $\text{LiOH} \cdot \text{H}_2\text{O}$  in a molar ratio of 1:1:3. Firstly, in a typical procedure,  $\text{FeSO}_4 \cdot 7\text{H}_2\text{O}$  aqueous solution was mixed with  $\text{H}_3\text{PO}_4$  under vigorous agitation. By drop wise addition of  $\text{LiOH} \cdot \text{H}_2\text{O}$  solution, a mass of sticky mixture was formed.

Polyethylene glycol (PEG: mean molecular weight of  $380\text{-}420 \text{ g mol}^{-1}$ ) was used, in four different experiments, in various concentrations of 2 vol. % (sample: LEG1), 8% (LEG2), 16% (LEG3) and 32% (LEG4). The pH values of solutions were adjusted to 7.14 by addition of NaOH. The resulting mixture was quickly transferred into 100-ml-capacity stainless steel autoclave lined with Teflon. The autoclave was sealed and the dead volume was purged with nitrogen to overcome undesired oxidizing reactions and kept at  $160 \text{ }^\circ\text{C}$  for 5h. Subsequently, the autoclave was cooled down to room temperature. Precipitate was collected by suction filtration, washed several times with deionized water, and dried in oven at  $100 \text{ }^\circ\text{C}$  for 3 h. To remove the adsorbed water, the LFP samples were heated at  $400 \text{ }^\circ\text{C}$  for 4 h under flowing  $\text{H}_2/\text{N}_2$  atmosphere (5 vol. %  $\text{H}_2$  and 95 vol. %  $\text{N}_2$ ).

### 2.2. Preparation of $\text{LiFePO}_4$ electrode

The cathode performance of LEG samples was evaluated by using a galvanic cell, which was assembled in a glove box filled with an argon atmosphere. The electrode was composed of  $\text{LiFePO}_4$  powder, graphite and PTFE in a weight ratio of 7.5:2.0:0.5. Lithium plates, cut from lithium metal ingots, were used for both negative and reference electrodes. The electrolyte was  $\text{LiClO}_4$  dissolved in a 1:1 weight ratio mixture of ethylene carbonate (EC) and dimethyl carbonate (DMC).

CV and EIS measurements were carried out by means of a galvanostat/potentiostat auto lab (PGSTAT 302N) at room temperature. The applied frequency range in EIS was 10 mHz to 1 MHz and the oscillation voltage was 50 mv. CV measurements were performed in a potential range of 2.5-4.5 V at scanning rate of  $0.1 \text{ mV} \cdot \text{s}^{-1}$ . The electrochemical charge-discharge measurements were carried out in the voltage range from 2.5 to 4.5 V *vs.*  $\text{Li}^+/\text{Li}$ .

### 2.3. Analytical measurements

The iron (III) concentration in  $\text{LiFePO}_4$  samples measured by the spectrometric method using 1,10-phenantroline. Iron (II) reacts with three O-phenantroline bidentate ligands to form a stable, red complex whose absorbance can be measured. Iron (III) sample must be first converted to iron (II) by

using a solution of 10% hydroxylamine hydrochloride ( $\text{NH}_2\text{OH} \cdot \text{HCl}$ ). About 100 mg  $\text{LiFePO}_4$  was used and dissolved in the mixture of 15 ml 1 M  $\text{H}_2\text{SO}_4$  and 10 ml 5 M  $\text{H}_3\text{PO}_4$  solution. In a 100 ml flask, 10 ml analyzed sample is introduced then 1 ml of 1.4 M hydroxylamine hydrochloride, 10 ml of 5 mM 1,10-phenanthroline and 8 ml of 1.2 M sodium acetate (as a buffer) were added and followed to stand for 15 minutes. The absorbances has been read at 508 nm. Iron (III) is calculated by subtracting the mg/L iron (II) from the mg/L total iron. A series of freshly prepared working standard ferrous iron solutions (up to 6 ppm iron) were treated similarly and the absorbance measured. Calibration curve was plotted with concentrations of different standard iron solutions against absorbance and the iron content of the unknown lithium iron phosphate samples is evaluated. The characteristics of iron calibration curves are: concentration range from 0.5 to 5.00 mg/L with a correlation coefficient of 0.9980.  $\text{Li}^+$  was determined by flame photometer in air/butane as fuel using an aqueous standard calibration curve. Analyses were made in triplicate and the mean values are reported.

#### 2.4. Characterization techniques

X-ray diffraction (XRD) measurements were carried out on a Bruker D8 Advance X-ray diffraction using  $\text{Cu K}\alpha$  radiation source ( $\lambda=1.540560 \text{ \AA}$ ) with a step size of  $0.031 \text{ min}^{-1}$  from  $15^\circ$  to  $65^\circ$ . Morphology of the product was observed with a scanning electron microscopic (SEM) using a Nihon Denshi JSM-5800 system.

Absorbance measurements were made on a Philips PU 8700 UV-visible single-beam spectrophotometer with a 1 cm glass cell. A flame photometer (model PFP7), equipped with air-butane as fuel, was used for the determination of lithium content in  $\text{LiFePO}_4$  samples.

### 3. RESULTS AND DISCUSSION

Fig.1 shows the X-ray diffraction patterns of samples prepared hydrothermally by using polyethylene glycol as the template and carbon source. By following the evolution of the XRD patterns as a function of the PEG concentration, we observed that the olivine structure was retained. All the diffraction peaks identified to be those from orthorhombic olivine-type structure with the space group of Pnma. LEG1 shows an impurity peak, which is speculated as characteristic peaks of  $\text{Fe}_2\text{O}_3$ . The peaks in the XRD patterns became sharper and the full-width at half-maximum (FWHM) decrease with the increase of PEG content in the precursor solutions, indicating better crystallization of LEG3 and LEG4. The latter materials exhibit no iron oxide impurities in the XRD patterns due to higher amount of PEG used in the corresponding precursor solution. Moreover, the PEG adsorbed on the surface of LEG particles, could passivate them against oxidation to some extent, which might be another possible reason that no Fe oxides or hydroxide were formed in both LEG3 and LEG4 samples. The well crystalline LEG4, with narrow and sharp diffraction peaks, have the highest Li/Fe atomic ratio. Table 1 shows the  $\text{Fe}^{3+}$  weight percent's and  $\text{Li}^+$  concentrations determined for LEG samples.

**Table 1.** Preparation conditions and chemical compositions of the LEG samples

Samples	PEG (ml)	Li (ppm)	Fe <sup>3+</sup> (wt. %)	Li/Fe
LEG1	2	3.933	0.96	0.889
LEG2	8	3.987	0.56	0.904
LEG3	16	4.021	0.45	0.912
LEG4	32	4.16	0.28	0.943

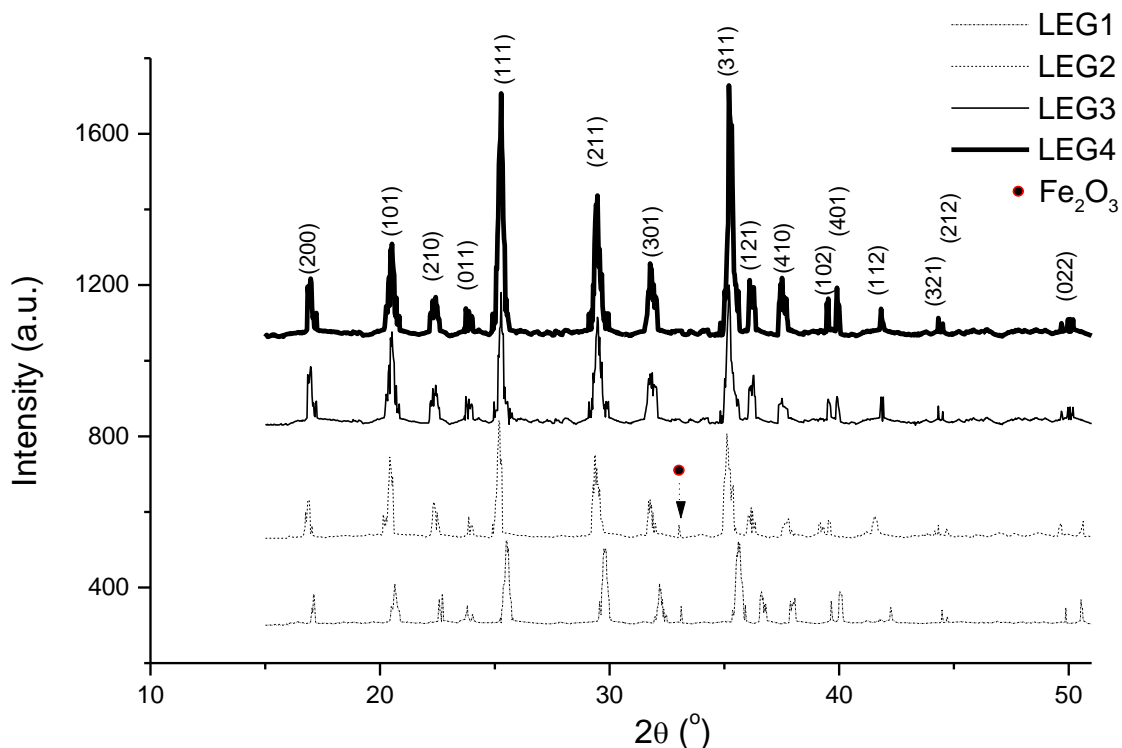
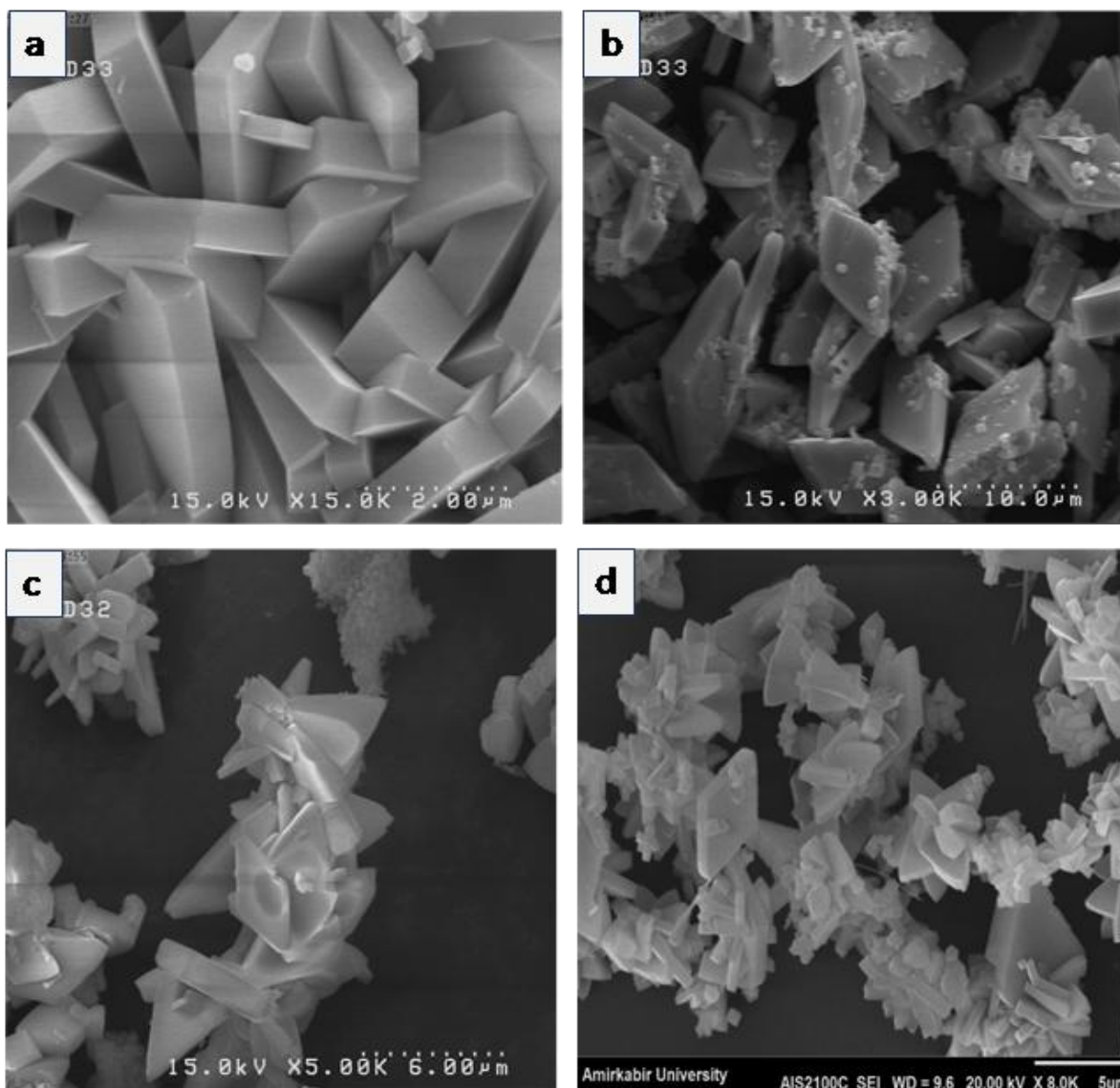
**Figure 1.** X-ray powder diffraction patterns of the LEG samples.

Fig. 2 show that large quantities of LiFePO<sub>4</sub> platelets of quadrangular (square and rhombic) are formed .LEG1 exhibits compact aggregates of rectangular platelets with a uniform thickness (Fig. 2a). The platelets are smooth in both a thickness of 800 nm and a length up to 3 μm. With an increase of the quantity of PEG in the precursor solution, the surface morphology turned from rectangular to single crystals with well-developed rhombohedral morphology (Fig.2b). Compared to LEG1, the average particle size and thickness of LEG2 decreased, where as its porosity is increased. The existence of pores shows that the material is not densely compacted between the platelets.

After further addition of PEG to the starting solution, the rhombohedral morphology is globally retained although particles are broken into small crystallites. Higher PEG concentration scan give a high viscosity to the solution provided by strong hydrogen bonds between hydroxyl groups of PEG. The cations in the solution may be trapped in the network of the hydrogen bonds. Such situation should promote nuclear generation and depress the crystal growth [14]. This phenomenon gave rise to rhombic morphology with truncated corners or some breakage of the edges (Figs.2c and 2d).SEM

shows that the increase in PEG concentration does not change the rhombohedral morphology of LEG3 and LEG4 samples.



**Figure 2.** SEM micrographs of a) LEG1, b) LEG2 ,c) LEG3 and d) LEG4 samples, prepared by hydrothermal method followed by heating in  $H_2/N_2$  atmosphere (5 vol.%  $H_2$  and 95 vol.%  $N_2$ ) at  $400^\circ C$  for 4h.

Generally, the hydrothermal process is controlled by the dissolution/recrystallization mechanism. If the probability of the crystal nucleation is higher than that of the crystal growth, the crystals will be small; otherwise they will be large. Obviously, the morphology and particle size of  $LiFePO_4$  is also dependent on PEG concentrations. Increasing PEG concentration should lead to smaller particles, because of the greater number of seeds forming and their smaller critical radius [15]. Evidently, with an increase in PEG concentration, the dissolution/recrystallization during the hydrothermal reaction became more vigorous, facilitating a fast nucleating process and hence formation of large numbers of crystal nuclei, which resulted in smaller particles.

As could be seen in voltammograms of  $\text{LiFePO}_4$  electrodes (Fig. 3), LEG4 exhibits the highest peak current densities among other samples, which could be partly attributed to a decrease in particle size of the obtained rhombohedral microcrystals. The potential separation between the two peaks increased in the order: LEG1:0.69 V > LEG2:0.53 V > LEG3: 0.47 V > LEG4:0.34 V. In the latter sample, the decrease of separations between the cathodic and anodic peaks is representative of its excellent kinetics and electrochemical reaction reversibility. The enhanced intercalation/de-intercalation kinetics of the latter could also be due to more availability of conductive carbon as a result of higher concentration of PEG used in the corresponding precursor solution. The largest peaks broadening of LEG1 could be attributed to its slower kinetics, indicating that the electrochemical behavior is controlled by the diffusion step.

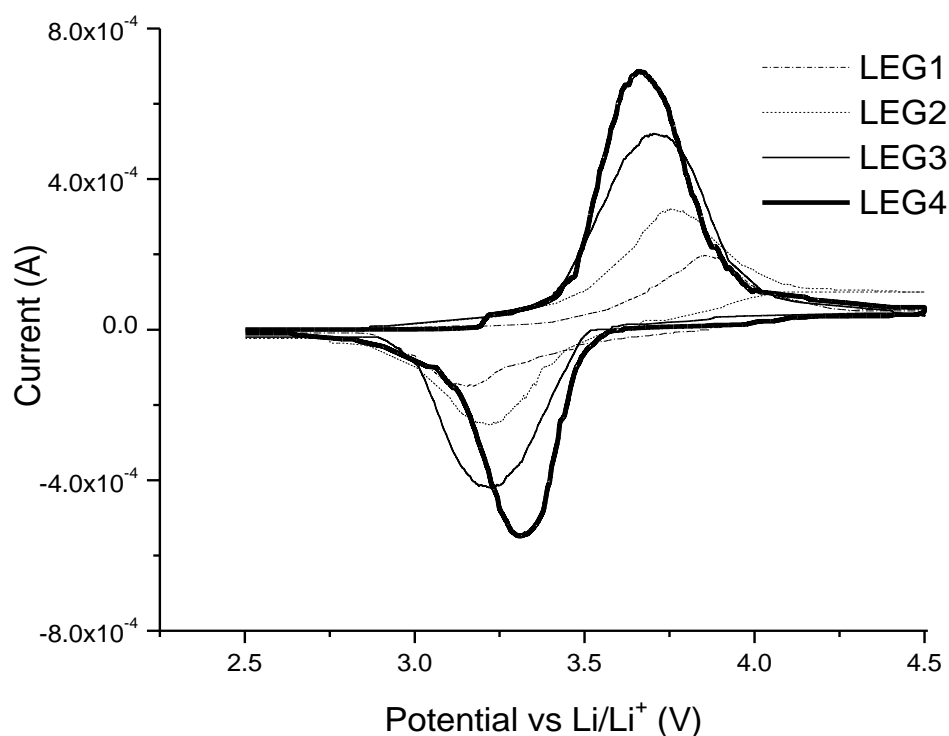


**Figure 3.** Cyclic voltammograms of LEG samples in the first cycle at a scan rate of  $0.1 \text{ mV s}^{-1}$  between the potential limit of 2.5 and 4.5 V (versus  $\text{Li}^+/\text{Li}$ )

Nyquist plots (Fig. 4) are composed of a semicircle in the high frequency related to the charge-transfer resistance  $R_{ct}$  of the  $\text{Li}^+$  ions at the  $\text{LiFePO}_4$ /electrolyte interface. This is followed by an inclined Warburg line in the low-frequency region, which is related to porous nature of cathode and diffusion of lithium ions within interior of the solid structure. The values of charge transfer resistance ( $R_{ct}$ ), estimated from diameters of semicircles on Nyquist plots, decrease in the order LEG1:  $629.49 \Omega$  > LEG2:  $530.55 \Omega$  > LEG3:  $351.42 \Omega$  > LEG4:  $267.42 \Omega$ . Since the charge-transfer reaction rate is proportional to the activity of metal ions, we may conclude that the rate of battery charging and discharging is enhanced by the addition of PEG, as in the case of LEG4.

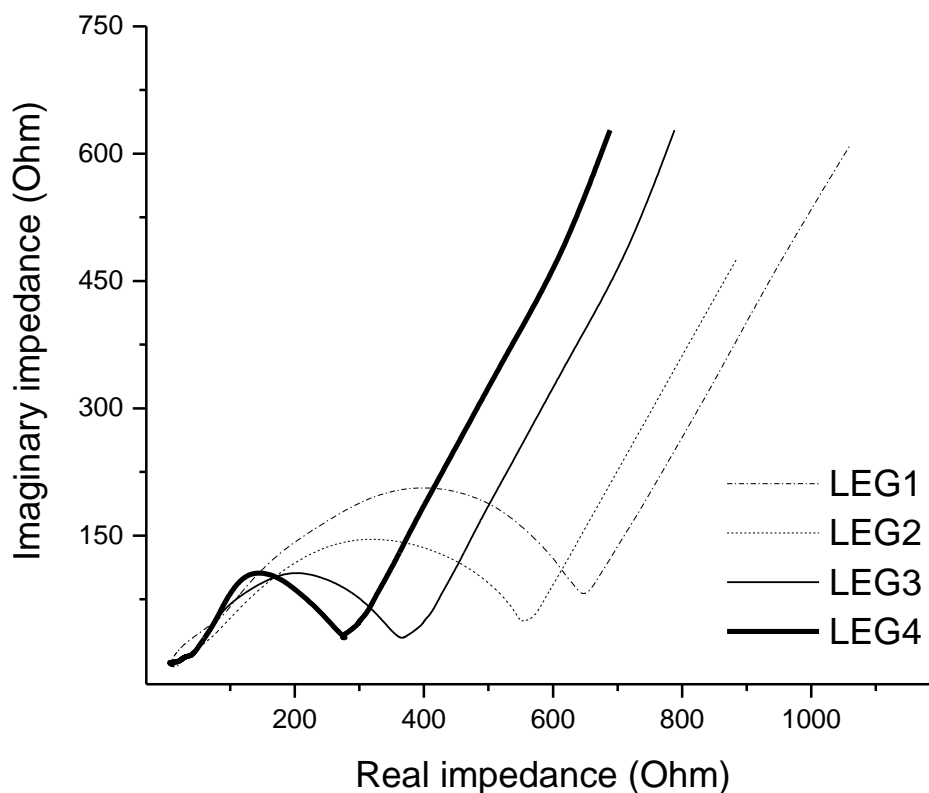
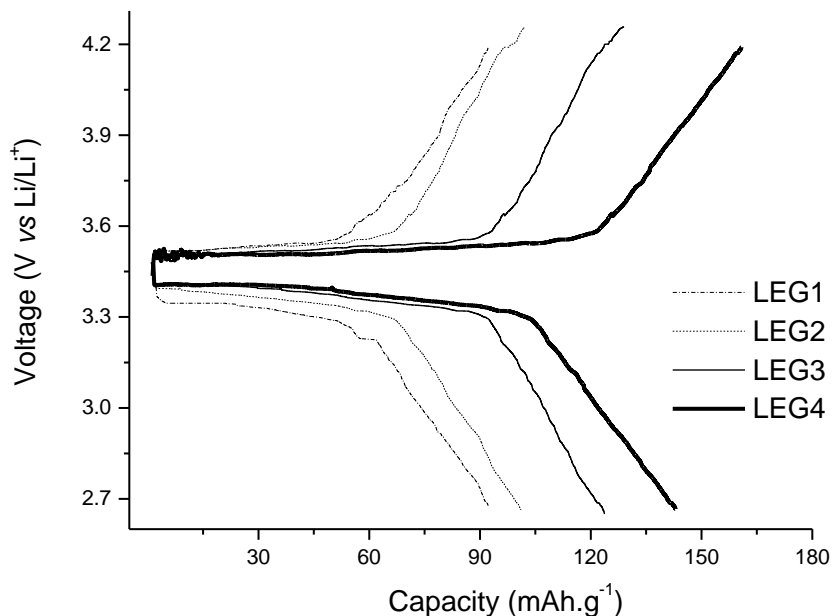


**Figure 4.** Electrochemical impedance spectroscopy (EIS) of LEG samples in the frequency range between 1 MHz and 10 mHz.

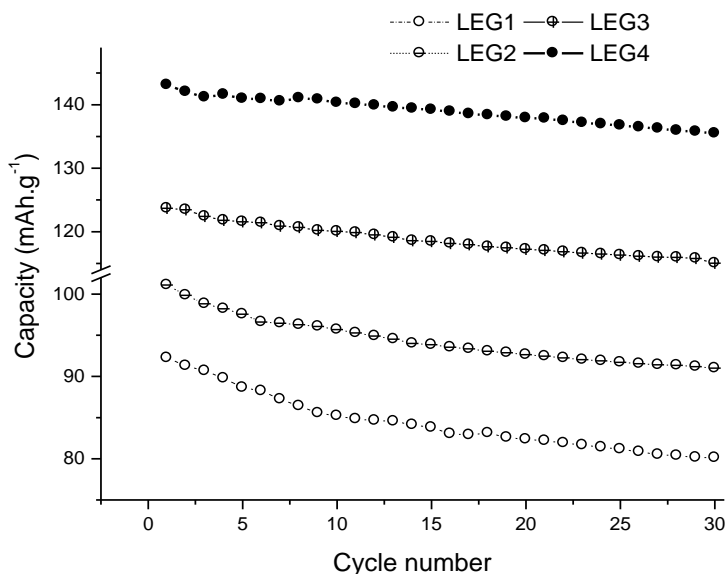
The first cycle charge-discharge curves of  $\text{LiFePO}_4$  samples are shown in Fig. 5. All these samples showed a good flat discharge voltage at approximately 3.4 V, which represent the typical intercalation/deintercalation of  $\text{Li}^+$  into the cathode crystal lattice. LEG1 showed a rather poor electrochemical behavior with the initial discharge capacity of about  $92 \text{ mAh.g}^{-1}$ . This phenomenon could be attributed to a possible lower amount of incorporated carbon and the effect of iron oxide impurities. During lithium intercalation, all the iron in  $\text{FePO}_4$  units is in the  $2^+$  oxidation state while that in  $\text{Fe}_2\text{O}_3$  remains in the  $3^+$  oxidation state, which is electrochemically inactive. With decreasing particle size from LEG2 to LEG4, the initial discharge capacity increased from 101 to  $143 \text{ mAh/g}$ . The latter, gives the highest initial discharge capacity of  $143 \text{ mAh g}^{-1}$ , which corresponds to over 84.12 % of the theoretical capacity of olivine  $\text{LiFePO}_4$ .

Fig. 6 shows the cycling performance of LEG electrodes between 2.5 V and 4.5 V windows at C/10 discharge rate up to the 30 cycles. LEG4, LEG3 and LEG2 exhibit good capacity retention of 94.7%, 93% and 90% of their initial capacities, respectively, whereas LEG1 shows 86.9% of its initial capacity. Fig. 6 clearly showed that the capacity of the LEG1 was decreased faster than the other samples.





**Figure 5.** Initial charge/discharge curves of LEG samples measured at a current density of 0.1 C in the potential range from 2.5 to 4.5 V.



**Figure 6.** Discharge capacities of the LEG samples as a function of cycle numbers.

#### 4. CONCLUSION

Phospho-olivine  $\text{LiFePO}_4$  microcrystals were successfully prepared by a simple hydrothermal synthesis route. It provides a facile method for the preparation of  $\text{LiFePO}_4$  cathode materials with well-developed rhombohedral morphology. Synthesis was carried out in the presence of poly ethylene glycol, which acts as a carbon source, structure oriented agent and surface-modifying reagent. The

concentration of polyethylene glycol in the precursor solution has great influence on the size and morphology of LiFePO<sub>4</sub>. Results confirm that PEG addition does not affect the structure of the cathode but considerably improves its kinetics in terms of capacity delivery. We may conclude that the size of the growing crystallites could be easily controlled by varying the PEG concentration, which spatially confined LiFePO<sub>4</sub> crystal growth. This enhancement could also be attributed to an increase in the electronic conductivity of intra- and inter-particles due to residue carbon. The preliminary data obtained in this work show that further optimizing of the preparation conditions may result in more precise control of the LiFePO<sub>4</sub> growth kinetics

#### ACKNOWLEDGEMENTS

Iran National Science Foundation (INSF) is gratefully acknowledged for financial support of this work.

#### References

1. J. Tollefson, T. Scully, A. Witze and O. Morton, *Nature* 454 (2008) 816
2. D. Lindley, *Nature* 463 (2010) 18
3. A. K. Padhi, K. S. Nujundaswamy and J. B. Goodenough, *J. Electrochem. Soc.* 144 (1997) 1188
4. A. S. Andersson, J. O. Thomas, B. Kalska and L. Haggstorm, *Electrochem. Solid-State Lett.* 144 (1997) 1188
5. S. T. Myung, S. Komaba, N. Hirosaki, H. Yashiro and N. Kumagai, *Electrochim. Acta* 9 (2004) 4213
6. Y. Jingsi and J. X. Jun, *Electrochem. Solid State Lett.* 7 (2004) 515.
7. S. F. Yang, P. Y. Zavalij and M. S. Whittingham, *Electrochem. Commun.* 3 (2001) 505
8. J. Chen, M. J Vacchio, S. Wang, N. Chernova and P. Y. Zavalij, *Solid state Ion.* 178 (2008) 1676
9. K. Dokko, H. Nakano and K. Kanamura, *Mater. Chem.* 17 (2007) 4803
10. K. Shiraishi, K. Dokko and K. Kanamura, *Power sources* 146 (2005) 555
11. G. Meligarana, C. Gerbaldi, A. Tuel and S. Bodoardo, *Power sources* 160 (2006) 516
12. B. Ellis, W. H. Kan, W. R. M. Makahnouk and L. F. Nazer, *Mater. Chem.* 17 (2007) 3248
13. A. Kuwahara, S. Suzuki and M. Miyayama, *Ceram. Int.* 34 (2008) 863
14. S. Tajimi, Y. Ikeda, K. Uematsu, K. Toda and M. Sato, *Solid State Ion.* 175 (2004) 287
15. N. Recham, L. Dupont, M. Courty, K. Djellab, D. Larcher, and M. Armand, J. M. Tarascon, *Chem. Mater.* 21 (2009) 1096